PLUTO'S INTERACTION WITH THE SOLAR WIND

FRAN BAGENAL
University of Colorado

THOMAS E. CRAVENS
University of Kansas

JANET G. LUHMANN
University of California at Los Angeles

and

RALPH L. McNUTT, Jr. and ANDREW F. CHENG
Johns Hopkins University, Applied Physics Laboratory

The two critical quantities that define the nature of Pluto's interaction with the solar wind are the degree of magnetization of the planet and the atmospheric escape rate. While it is not considered likely that Pluto has an internal magnetic dynamo, it is possible that some remanent magnetization is present. Because of the weak solar wind, even weak magnetization (20 nT at the planet's surface) would result in an appreciable magnetosphere. In the case of no magnetization, if Pluto's atmospheric escape rate is significantly greater than 1.5×10^{27} molecules s^{-1} then the interaction with the tenuous solar wind at 30 AU will be like that of a comet; there will be an extensive ion pickup upstream and the size of the interaction region will vary in proportion to variations in the solar wind flux. If the escape flux is less than 1.5×10^{27} molecules s^{-1}, then one expects that the solar wind will be at least partially deflected around Pluto's ionosphere in a more Venus-like interaction or absorbed in a lunar-like interaction. In either case, the gyroradii of both solar wind ions and atmospheric ions picked up will be very large due to the weak interplanetary magnetic field at 30 AU leading to significant kinetic effects. Strong temporal variations are expected in the nature of the interaction on time scales of days (due to changes in the solar wind) and over Pluto's orbit (due to changes in Pluto's atmosphere). Charon probably lacks both sufficient atmosphere and sufficient conductivity to have a significant effect on the plasma in which it is embedded and simply absorbs the impinging solar wind or magnetospheric plasma.

I. INTRODUCTION

The first mention of a possible interaction of Pluto with the solar wind was made in the context of possible Grand Tour trajectories by Dryer et al. (1973), who modeled the interaction as that of an unmagnetized planet with a van-

ishingly thin ionosphere. While Dessler and Russell's original proposal that Pluto is like a comet was made partly in jest (Dessler and Russell 1980), the recent observations of Pluto's atmosphere (Hubbard et al. 1988; Elliot et al. 1989) and spacecraft measurements of the solar wind at 30 AU now allow us to examine seriously this possibility. Pluto's low gravity implies that its atmosphere is only weakly bound and the escape rate may be high. Bagenal and McNutt (1989) considered the upper limits placed on the escape rate by various models (Hunten and Watson 1982; Hubbard et al. 1990; McNutt 1989) and explored the consequences for the solar wind interaction. In the case of high atmospheric escape rates, we expect a comet-like interaction with significant mass loading of the solar wind over an extensive region around Pluto. This mass loading is due to ion pickup following the ionization of the outflowing neutral molecules. For the case of low atmospheric escape rate, we consider whether Pluto's ionosphere could deflect the solar wind in a Venus-like interaction confined to a region much closer to the planet. A very weak atmosphere could lead to complete absorption of incident plasma, as at the Moon, and the production of a sputtered exosphere.

Although Triton bears some similarities to Pluto, Triton's atmospheric structure is quite different, resulting in a negligible thermal escape rate (see the chapter by Trafton et al.). The surrounding plasma environments are also quite dissimilar. Triton is always immersed in the tenuous (<0.01 cm^{-3}) and relatively hot ($\sim$100 eV) plasma of Neptune's magnetosphere (Richardson et al. 1995) as compared with the equally tenuous yet far colder ($T_{\rm ion}\sim 1$ eV) solar wind plasma at Pluto. In addition, the ambient magnetic field strength at Triton (5 nT) is significantly more than that in the solar wind (0.15 nT at Neptune during the Voyager 2 encounter). These two characteristics, a hotter and more-magnetized plasma at Triton, would result in significantly different interactions between these bodies and their environments even if their magnetization and outgassing rates were identical (cf., e.g., Neubauer et al. 1991). Titan, the other small world with a substantial atmosphere, interacts with the plasma in Saturn's magnetosphere which is even more strongly magnetized than that of Neptune. Hence, at the current epoch, the interaction of Pluto with the solar wind plasma is truly unique in the solar system.

Recent observations of magnetic signatures near Galileo's closest approach to asteroid Gaspra, interpreted as indications of appreciable remanent magnetization (Kivelson et al. 1993), have raised the possibility that Pluto too may be magnetized. If Pluto has a strong intrinsic magnetic field, then it will have a magnetosphere which persists throughout Pluto's orbit (i.e., is independent of the atmospheric escape rate), similar to the small magnetosphere of Mercury.

In this chapter, we first consider the solar wind conditions at 30 to 50 AU before exploring the possibilities and consequences of Pluto having an intrinsic magnetic field, the effects of Pluto's atmosphere on the solar wind interaction and the role of Pluto's satellite Charon. We then consider short- and long-term variability of the interaction. Finally, we consider how *in-situ* measurements of this unique plasma environment could be made from a spacecraft passing through the system.

II. SOLAR WIND AT 30 TO 50 AU

By 30 AU the solar wind has become a tenuous stream of cold particles (see Table I for properties; also see Belcher et al. 1993). The interplanetary magnetic field (IMF) has become wound up in the Parker spiral so that it is on average very close to azimuthal in direction and reduced to about 0.2 nT in magnitude. The solar wind plasma has cooled (to a few eV) so that the energy of the solar wind is mostly in its convective or bulk motion (i.e., the flow is highly supersonic [see Table I for relevant Mach numbers]). While the solar wind maintains a speed on the order of 450 km s^{-1}, the $1/R^2$-decreasing density has dropped to $\sim$0.01 cm^{-3} and the solar wind ram pressure is so weak (2×10^{-11} dyne cm^{-2}) that even small electrodynamic effects of the Pluto–Charon system can cause a significant perturbation of the solar wind. The gyroradii of solar wind protons and ionized atmospheric ions are comparable to the size of Pluto, but gross dynamic features, such as momentum balance, can be approximated in fluid models of the interaction.

TABLE I

Solar Wind at 30 to 50 AU

Parameter		Typical Value	Variability[a]
Magnetic field	B	0.2 nT	×2
Solar wind speed	$V_{\rm sw}$	450 km s^{-1}	±75 km s^{-1}
Proton density	$n_{\rm proton}$ at 30 AU	0.01 cm^{-3}	×2
	at 50 AU	0.004 cm^{-3}	
Ram pressure	$\rho {V_{\rm sw}}^2$	2×10^{-11} dyne cm^{-2}	×2
Proton temperature	T_i	1.3 eV	±0.4 eV
		15,000 K	±5000 K
Mach number	$M\equiv V_{\rm sw}/(2kT_i/m_p)^{1/2}$	~45	×2
Alfvén Mach number	$M_A\equiv V_{\rm sw}/(B^2/4\pi n_p m_p)^{1/2}$	~10	×2
Sonic Mach number	$M_S\equiv V_{\rm sw}/(kT_e/m_p)^{1/2}$	~30	×2
CH_4^+ gyroradius	$r_{pu}(CH_4^+)$	300,000 km≈300 $R_{\rm Pluto}$	
Proton gyroradius	$r_{\rm gyro}$(proton)	600 km	
Electron gyroradius	$r_{\rm gyro}$(electron)	10 km	
Bow shock width[b]	$r' = V_{\rm sw}/\Omega_{ci}$	23,000 km≈20 $R_{\rm Pluto}$	

[a] Changes that can be expected on a time scale of days (×2 means a factor of two).

[b] The effective gyroradius of upstream protons whose bulk motion ($V_{\rm sw}$) is converted to gyromotion at the shock (cf., Bagenal et al. 1987).

The first thing to consider is the nature of a bow shock that might form upstream of an obstacle such as Pluto, immersed in a highly supersonic and

collisionless flow and extremely weak magnetic field. Voyager 2 observations of Uranus' bow shock (Bagenal et al. 1987) and Neptune's bow shock (Richardson et al. 1995) confirmed theoretical expectations that the thickness of a high Mach number, quasi-perpendicular shock is of the order of $r' \sim V_{sw}/\Omega_{gyro}$ (where V_{sw} and Ω_{gyro} are the flow speed and gyrofrequency of the solar wind ions upstream of the shock). Even at perihelion, the ambient magnetic field strength at Pluto probably does not exceed 0.2 nT. At this strength, the shock thickness would be about 20 R_{Pluto} for protons (on the order of the stand-off distance) and would be even larger if there is a substantial amount of heavy ions picked up upstream. Under such conditions, a thick, disturbed region will form upstream of the obstacle where a bow shock would be expected in fluid models. Moreover, it is probable that over such a large distance the perturbations in the solar wind flow due to pickup of escaping atmospheric neutrals would be as strong as any effects of the electric and magnetic fields normally associated with a shock. These general issues have been reviewed by Galeev (1991).

Voyager 2 and Pioneer observations in the outer heliosphere show minor changes in average properties of the solar wind between 30 and 50 AU compared with the level of variability over a single solar rotation (Gazis et al. 1989; Belcher et al. 1993). Thus, any long-term systematic change in the interaction as Pluto moves from perihelion to aphelion will probably be dominated by changes in Pluto's atmosphere. But short-term variations may exceed the variations caused by the orbital motion.

III. MAGNETIC INTERACTION

A. Sources of Magnetization

While it is highly improbable that Pluto or Charon has a liquid metal core in which a magnetic dynamo (similar to the Earth's or Mercury's) might operate, it is remotely possible that significant convection in the ice mantle might generate a dynamo. It should be noted that scepticism about a Pluto dynamo is based on the lack of evidence of significant dynamo fields in the larger satellites of Jupiter and Saturn rather than on solid understanding of dynamo processes (cf., Kivelson et al. 1979).

A second possibility is that Pluto has significant remanent magnetization. Natural remanent magnetizations as high as 0.3 A m^2 kg^{-1} have been found in chondritic meteorites (Sugiura and Strangeway 1988) and a magnetization of 0.001 to 0.03 A m^2 kg^{-1} has been inferred for the asteroid Gaspra from magnetic perturbations measured during the recent Galileo flyby (Kivelson et al. 1993). For an upper limit to the remanent magnetization, we assume that Pluto has a rocky core that is magnetized to a level of 0.03 A m^2 kg^{-1}, comparable to the most magnetized chondritic meteorites and iron meteorites. Then for a core radius of 300 km and a density 2 g cm^{-3}, Pluto's magnetic moment would be 450 nT R_P^3, comparable in planetary units to that of Mercury. Alternatively, the core magnetization may be modeled as a large number of randomly oriented magnetic "domains" from accretion of magnetized bodies or from impact generation of magnetic fields. If, for example, there are 100 domains each with a modest 0.001 A m^2 kg^{-1} magnetization and assuming a density of 2 g cm^{-3}, and supposing all of these domains line up during accretion making Pluto a "magnetic rubble pile," then a global magnetic dipole moment of about 42 nT R_P^3 would result, which would produce an intrinsic magnetosphere. Here the domains are in analogy to the microscopic magnetic domains that are set up on intermediate scales (as in commonly found pieces of magnetized iron).

B. A Magnetosphere

The condition for a magnetosphere is that there is a region outside the planet where the magnetic field of the planet is strong enough to exclude the solar wind. The upstream magnetospheric boundary (the magnetopause) is approximately located where the pressure of the planet's magnetic field ($B_o^2/2\mu_o$) stands off the solar wind ram pressure ($\rho_{sw}V_{sw}^2$) at $R_{mp}/R_{planet} \sim (B_o^2/2\,\mu_o\,\rho_{sw}V_{sw}^2)^{1/6}$ (Siscoe 1979). Thus, the size of the magnetosphere relative to the planet is proportional to $B_o^{1/3}$.

For Pluto to have a magnetosphere (i.e., $R_{mp}/R_{Pluto} > 1$) the surface field needs to be $B_o > 1$ nT. Much greater magnetic fields are known to exist at Mercury (surface magnetic fields of 400–600 nT), the Moon (up to 327 nT at Apollo landing sites), and for many differentiated meteorites and even some carbonaceous chondrites (see references in Kivelson et al. 1993).

For the magnetosphere to extend to Charon's orbit at 17 R_{Pluto}, the surface field must be $B_o > \sim 3700$ nT. Even weak magnetization, therefore, would produce a magnetosphere. However, for the magnetic interaction with the solar wind to dominate over effects of ionizing the outflowing atmosphere (discussed below), Pluto would need to have either strong remanent magnetization or a dynamo. Such a magnetosphere (illustrated in Fig. 1) would be similar to Mercury's magnetosphere (see review by Russell et al. 1988) with no belts of trapped radiation but with plasma flows induced by the magnetic interaction with the solar wind. Unlike Mercury, substorm-like acceleration of charged particles would not be significant in Pluto's magnetosphere. This is because the interplanetary magnetic field strength, and hence the solar wind convection electric field, is much weaker at Pluto due to the much greater distance from the Sun. Hence, the energy input into the magnetosphere and cross tail potential are also much less (M. G. Kivelson, personal communication, 1993). This magnetosphere would persist throughout Pluto's orbit, even when Pluto's atmosphere has turned to surface frost. Only after much of the atmosphere had condensed out would any moderately energized magnetospheric ions and electrons be able to penetrate through the atmosphere to the surface (this process is difficult to quantify because the particle penetration is a function of energy).

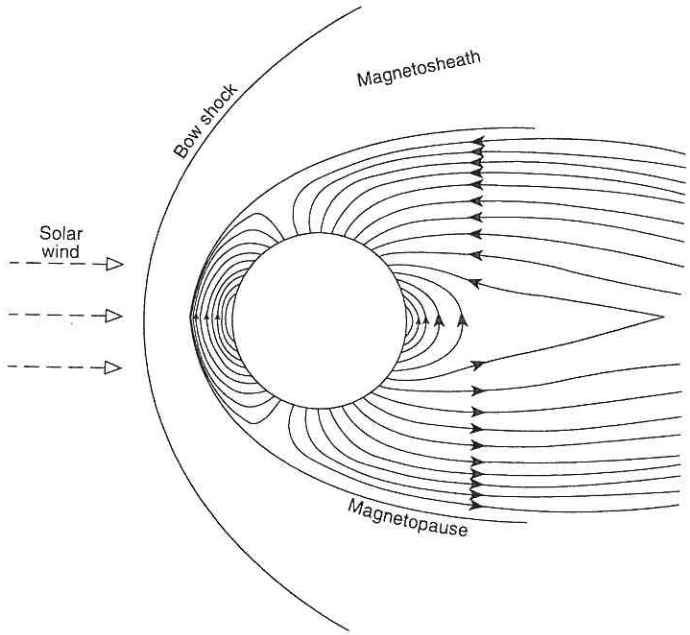

Figure 1. Sketch of the interaction of Pluto with the solar wind for the case of Pluto having an intrinsic magnetic field. The solid (dashed) arrows show magnetic field lines (solar wind flow).

IV. COMET-LIKE INTERACTION

The 1988 stellar occultation of Pluto confirmed the existence of a substantial atmosphere and provided a measure of the density profile between 1500 and 1200 km from the center of the planet (Hubbard et al. 1988; Elliot et al. 1989). The nature of Pluto's outer atmosphere, however, remains an important issue (see the chapters by Yelle and Elliot, Summers et al., and Trafton et al.).

In 1980, Trafton speculated that the spectroscopic identification of CH_4 frost on Pluto implied an atmosphere composed of gases heavier than CH_4; otherwise CH_4 ice would have sublimated away, reducing Pluto's mass appreciably over cosmogonic time scales (Trafton 1980). Hunten and Watson (1982), criticizing Trafton's assumption of an isothermal atmosphere, applied studies of hydrodynamic escape for the early atmospheres of the Earth and Venus (Watson et al. 1981) and derived a substantially lower removal rate. In the Watson et al. model the escape of material from the upper atmosphere is limited by the rate at which the upper atmosphere can be heated (by solar EUV or the interaction with the solar wind) to offset cooling due to expansion. Hunten and Watson (1982) inserted pre-occultation estimates of the properties

of Pluto's atmosphere into the Watson et al. formulation to obtain upper limits on Pluto's escape flux of 1 to 6×10^{28} molecules s^{-1}. Trafton et al. (1988) calculated that the same atmospheric escape process on Charon could have completely removed any atmosphere and volatile surface ices, explaining the apparent absence of volatiles on Charon's surface. Reconsidering the issue of hydrodynamic escape in light of the occultation results, Hubbard et al. (1990) pointed out that the low solar EUV flux at Pluto may mean that the escape flux may not be controlled so much by the thermal structure *below* the region of EUV heating as *above* it. The situation would then be analogous to the solar wind, as described by Parker (1964). Hubbard et al. (1990) derived upper limits for the escape rate of 3.4×10^{28} molecules s^{-1} for the Watson et al. formulation and 1.2×10^{28} molecules s^{-1} for a Parker-type wind. However, McNutt (1989) pointed out that Hubbard et al.'s use of the isothermal formula for the altitude of unit optical depth (λ_1, in terms of the local scale height) is inappropriate and probably an overestimate of the actual escape rate. Calculating λ_1 and the escape flux self-consistently, McNutt (1989) derived values as low as 2.3×10^{27} molecules s^{-1}, depending on the efficiency of the solar EUV heating of the atmosphere. Trafton's (1990) numerical model produced comparable values.

Recent detections of N_2, CO and CH_4 ice on Pluto's surface by Owen et al. (1993) imply that the atmosphere is dominated by N_2 with about a percent each of CH_4 and CO. Trafton et al. (see their chapter) discuss why these volatiles should be hydrodynamically escaping with fluxes in proportion to their mole fractions in the pristine ice reservoir (which continually replaces the escaping atmosphere).

A. Upstream Pickup Ions

Exospheric neutral atoms and molecules (such as CH_4) that escape from Pluto form a tenuous "cloud" that extends into interplanetary space for millions of km. The chance of a collisional interaction between these neutrals and the solar wind plasma is very small because of the low number densities. Eventually, the neutral atoms and molecules are ionized by solar EUV photons or by charge transfer collisions with solar wind protons. For example, CH_4^+ ions are created in the solar wind by the reaction:

$$h\nu + CH_4 \rightarrow CH_4^+ + e. \quad (1)$$

Once an ion has been created, then it feels and reacts to the solar wind. More specifically, the ion responds to the Lorentz force, $\mathbf{F} = q(\mathbf{E} + \mathbf{v} \times \mathbf{B})$, where $\mathbf{v}$ is the particle velocity, q is the ion charge, $\mathbf{B}$ is the interplanetary magnetic field and $\mathbf{E}$ is the motional electric field $\mathbf{E} = -\mathbf{V}_{sw} \times \mathbf{B}$, where $\mathbf{V}_{sw}$ is the solar wind flow velocity relative to the escaping neutral.

The newly born ion is initially created at the neutral's escape speed V_{esc}, which is much less than the solar wind speed (i.e., $V_{esc} \ll V_{sw}$), but the electric field quickly accelerates the new ion. The $\mathbf{E}$ and $\mathbf{B}$ fields are approximately

uniform and the resulting ion trajectories are cycloidal. The ions thus start to move along with the solar wind and are referred to as pickup ions. The new electron "sees" the same electric field and is also accelerated, but because of its small mass it has a correspondingly smaller gyroradius and pickup energy.

This type of ion motion was observed in the solar wind near comets Halley, Giacobini-Zinner (G-Z) and Grigg-Skjellerup (G-S) (cf., Neugebauer 1990; Galeev 1991; Coates et al. 1993*a,b*). Kecskemety and Cravens (1993) have simulated pickup ions from atmospheric escape at Pluto and Fig. 2 shows their calculated trajectories of methane ions in the solar wind upstream of Pluto. These ions were created randomly (at rest) with a probability that decreased with increasing distance from Pluto. This is because the ion production rate is proportional to the neutral density which varies inversely as the square of the radial distance.

The ion velocity for this type of motion can be represented as the sum of gyromotion about the magnetic field in the solar wind reference frame plus an $\mathbf{E} \times \mathbf{B}$ drift motion. The ion gyrofrequency is given by:

$$\Omega_{\text{gyro}} = qB/m. \tag{2}$$

For methane ions near Pluto, $\Omega_{\text{gyro}} \approx 10^{-3}$ radian s^{-1}. The gyroradius for methane pickup ions is then given by the expression:

$$r_{\text{gyro}} = V_{\text{sw}}/\Omega_{\text{gyro}} \approx 3 \times 10^5 \text{ km} \approx 250 \text{ R}_{\text{Pluto}}. \tag{3}$$

Molecular nitrogen ions (or carbon monoxide ions which also have a mass of 28 amu) will have pickup gyroradii roughly twice as large. The typical scale of the trajectories in Fig. 2 is indeed the gyroradius, which obviously greatly exceeds the radius of Pluto. The gyroradius also is much greater than the distance to the bow shock (R_{bs}). The fact that $r_{\text{gyro}} \gg R_{\text{bs}} \geq \text{R}_{\text{Pluto}}$ is a strong indicator that the solar wind interaction with Pluto, at least at large distances, is strongly kinetic rather than fluid so that one must be extremely cautious about applying fluid-based methods such as magnetohydrodynamics to this problem. Near the planet the gyroradii will decrease somewhat as the magnetic field is compressed by the "obstacle" formed by the pickup process and the MHD approach is more appropriate.

In the outer heliosphere the IMF is almost orthogonal, on average, to the solar wind direction, in which case the drift velocity is just equal to the solar wind velocity and the gyration speed is equal to V_{sw}. A maximum ion speed of $2V_{\text{sw}}$ is then attained at the top of the cycloidal trajectory. The kinetic energy of a pickup methane ion is about 10 keV in the solar wind frame, but the maximum energy in the Pluto frame is $E_{\text{max}} \approx m(2V_{\text{sw}})^2/2 \approx 40$ keV. Pickup molecular nitrogen would be almost twice as energetic even though the field fluctuations are comparable to the background field in magnitude. Figure 3 is a diagram of velocity space from Kecskemety and Cravens (1993) for a distance upstream of Pluto of 10^5 km. The type of ion distribution

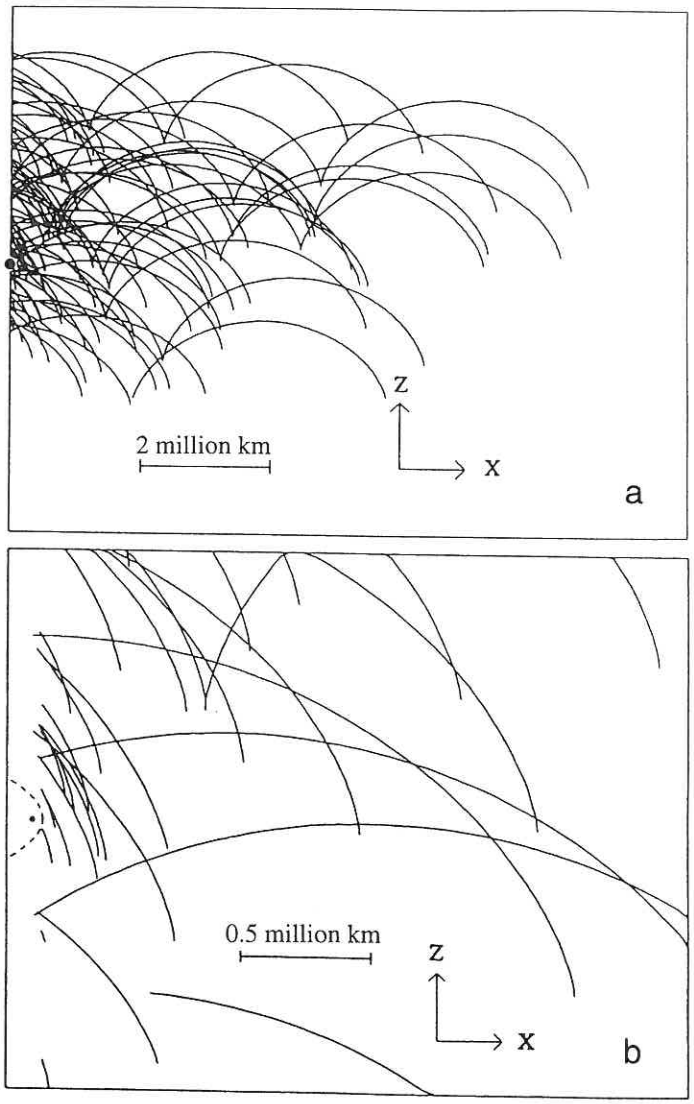

Figure 2. (a) Calculated trajectories of pickup CH_4 ions. Pluto is shown as the large dot on the left side of the plot and the solar wind flow is from the right to left. The x-axis points from Pluto to the Sun. The interplanetary magnetic field is directed in the y-direction (into the page). The CH_4 ions are created at rest but they move towards Pluto on cycloidal trajectories. (b) Expanded view of (a). Pluto is shown as a dot and the estimated location of a possible bow shock is indicated by the dashed line. The trajectories were stopped at the y-z plane containing Pluto (figure from Kecskemety and Cravens 1993).

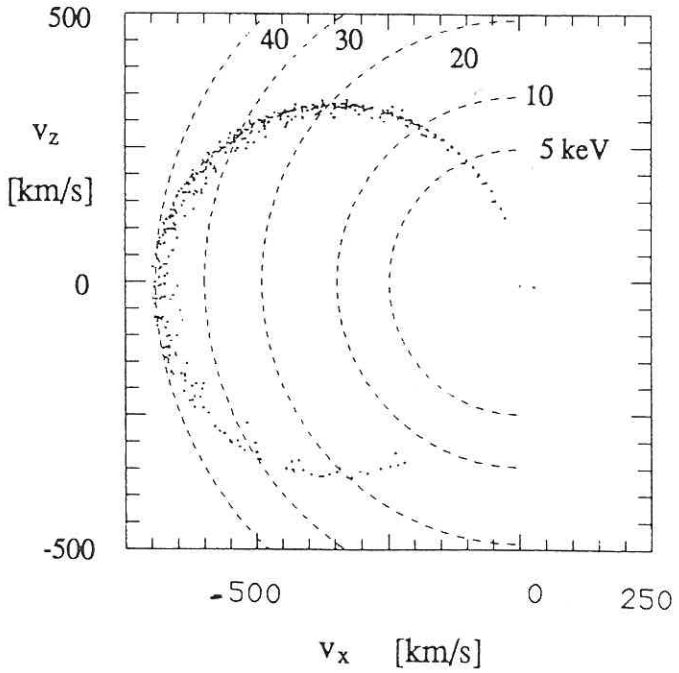

Figure 3. Scatter plot in the $Vx - Vz$ velocity space (in the Pluto reference frame) of calculated CH_4 pickup ion velocity vectors at a distance of 10^5 km upstream of Pluto. The pickup ions are clearly of the form of a ring distribution. The center of the ring is the solar wind velocity. Circles of constant energy for CH_4 ions (in keV) are indicated by the dashed lines. For this calculation, Kecskemety and Cravens (1993) included magnetic fluctuations (of magnitude 0.3× background) propagating away from Pluto (in the solar wind reference frame) and solar wind fluctuations (of magnitude comparable to the background field) propagating towards Pluto (figure from Kecskemety and Cravens 1993).

shown is what one would expect from cycloidal trajectories. This type of distribution is known as a ring distribution and was studied for the solar wind interaction with comets (cf., Galeev 1991). The center of the ring is the solar wind velocity vector, and the radius is the solar wind speed.

Actually, the calculations for Fig. 3 also included the effects of fluctuations, or waves, in the magnetic field, which scatter the ions such that they no longer execute "perfect" cycloidal motion, or form a perfect ring distribution in velocity space. Magnetic fluctuations or waves are originally present in the solar wind and are also generated by plasma instabilities associated with the presence in the solar wind plasma of a ring (or ring/beam) distribution of contaminant heavy ions (Wu and Davidson 1972; Sagdeev et al. 1986; Glassmeier and Neubauer 1993; Neubauer et al. 1993*a,b*; Glassmeier et al. 1993; Motschmann and Glassmeier 1993; Coates et al. 1993*a,b*; Huddleston et al. 1993). However, the deviation of the calculated distribution function from a ring in Fig. 3 is quite small. Kecskemety and Cravens (1993) concluded that magnetic fluctuations probably are not important for the solar wind interaction with Pluto. In this sense the solar wind interaction with Pluto is different from the cometary interaction, because it has been shown for the latter that particle scattering by magnetic fluctuations is very important. In fact, in the region near cometary bow shocks the ring distributions are converted to spherical shell distributions by wave-particle interactions. The main reason for this difference between cometary and Pluto pickup ions is that most of the ions at a given location have executed less than a full gyration because of the extremely large ion gyroradius at Pluto. The pickup ions do not have enough time to be scattered by magnetic fluctuations. A second reason for the lower effectiveness of ion scattering at Pluto relative to comets is that the pitch angle of the pickup ions at Pluto is close to 90 degrees where scattering is less efficient (due to the quasi-linear diffusion gap; Galeev 1987), whereas the initial pitch angles for cometary pickup ions are much smaller.

Another difference between the solar wind–comet interaction and the Pluto case is evident in Fig. 3. For active comets, the ring distribution (at least until the ring distribution is converted to a shell distribution) is expected to be populated almost evenly around the ring, whereas for Pluto the top part of the ring contains more ions. That is, the ion distribution function at Pluto is highly nongyrotropic. In other words, at any given location there are many more ions moving upward than moving downward. This is also apparent in Fig. 2 and is another indication that the solar wind interaction with Pluto is hard to describe in a fluid sense. Nonetheless, for lack of any better method we will still use the cometary analogy and fluid theory to try to understand the dynamics of the solar wind interaction with Pluto. Fortunately, in the region very close to Pluto the solar wind flow should be much slower and the interaction more fluid-like than what we have just discussed for the upstream region.

B. The Cometosphere

If Pluto has a large atmospheric escape flux, then one expects a comet-like interaction with significant mass loading of the solar wind due to the ionization of escaping neutrals. The size of the cometary interaction region was confirmed by *in-situ* observations of comets Halley and G-Z (Neugebauer et al. 1989) to be on the order of

$$R_{so} = \frac{\mu Q_{esc}}{4\pi V_{esc} \tau n_{sw} V_{sw}} \tag{4}$$

(see, e.g., Galeev et al. 1985) where μ is the molecular weight and Q_{esc} the total escape rate of neutrals, V_{esc} is the escape speed, τ is the ionization time scale, and n_{sw} and V_{sw} are the upstream solar wind density and flow speed. Note that for photoionization by solar radiation $\tau n_{sw} V_{sw}$ is approximately constant with radial distance from the Sun. For photoionization of methane

(to CH_4^+ or CH_3^+) at 30 AU $\tau \sim 1.2 \times 10^9$ s (Delitsky et al. 1989). Extrapolation of the ionization rates for CO given by Cravens et al. (1987) to 30 AU gives similar values. The corresponding time for N_2^+ is only slightly longer with $\tau \sim 1.6 \times 10^9$ (Yung and Lyons 1990). Thus, the following discussion is likely independent of the composition of Pluto's atmosphere. The escape speed of the neutral flow will be $V_{esc} \sim V_g/\sqrt{\lambda_1} \sim 0.4$ km s^{-1} where V_g is Pluto's surface escape speed (1.17 km s^{-1}) and we have taken $\lambda_1 \sim 10$ (McNutt 1989) (note that the escape flow speed is less than the surface escape speed due to the altitude of the escape in this model). Thus for methane ($\mu = 16$) the scale length becomes typically

$$\frac{R_{so}}{R_{Pluto}} = \frac{Q_{esc}}{Q_o} \tag{5}$$

where $Q_o = 1.5 \times 10^{27}$ molecules s^{-1}. Note that including charge exchange and impact ionization will decrease τ and make R_{so} larger (Cravens et al. 1987). Thus, an escape rate of $\sim 10^{28}$, which would be comparable to the outgassing of comet G-Z at 1 AU (Mendis et al. 1986) and consistent with upper limits derived by Hunten and Watson (1982), Hubbard et al. (1990), and the more optimistic cases of McNutt (1989), would produce $R_{so} \sim 6\, R_{Pluto}$.

The recent encounter of the Giotto spacecraft with comet G-S provides an example of mass loading at a value less than that of Halley and G-Z but comparable to that possible for Pluto. Huddleston et al. (1993) infer a mass injection rate of $Q = 7.5 \times 10^{27}$ molecules s^{-1}. The IMF had a relatively large value of 16 nT (Neubauer et al. 1993*a*,*b*) and the IMF angle with respect to the solar wind was close to 90 deg, which is what we expect for the IMF near Pluto. In fact, the pickup ion distributions measured at G-S are more ring-like than the distributions measured at comet Halley (Coates et al. 1993*a*,*b*). On the other hand, if Pluto is magnetized, the plasma flow pattern would be very different from that of a comet (modeling results for G-S cometary encounter are also discussed by Flammer and Mendis [1993] and by Schmidt et al. [1993]).

For comets, Galeev et al. (1985) derived the distance to the bow shock to be $R_s = \xi R_{so}$ where the factor ξ accounts for the effect of the shock on the flow and has a value of ~ 5 for a Mach 2 shock. The value of ξ is expected to increase with Mach number (Mendis et al. 1986), but the uncertainty in the nature of anything like a bow shock at Pluto makes it impossible to estimate the corresponding ξ factor. We can only conclude that the size of the interaction region will be very large, even for modest atmospheric escape rates.

Following the comet-like model, the interaction of the Pluto–Charon system with the solar wind is sketched in Fig. 4. At 17 R_{Pluto}, Charon's orbit will lie entirely inside the interaction region only under conditions of high escape flux or low solar wind flux. For example, if one takes $n_{sw} V_{sw} \sim 1.0 \times 10^5$ cm^{-2} s^{-1} (1σ below the average reported by Villanueva et al. [1989]), then an escape flux of 7×10^{27} molecules s^{-1} is required to make $R_{so} > 17\, R_{Pluto}$ and hence include both bodies in the interaction region.

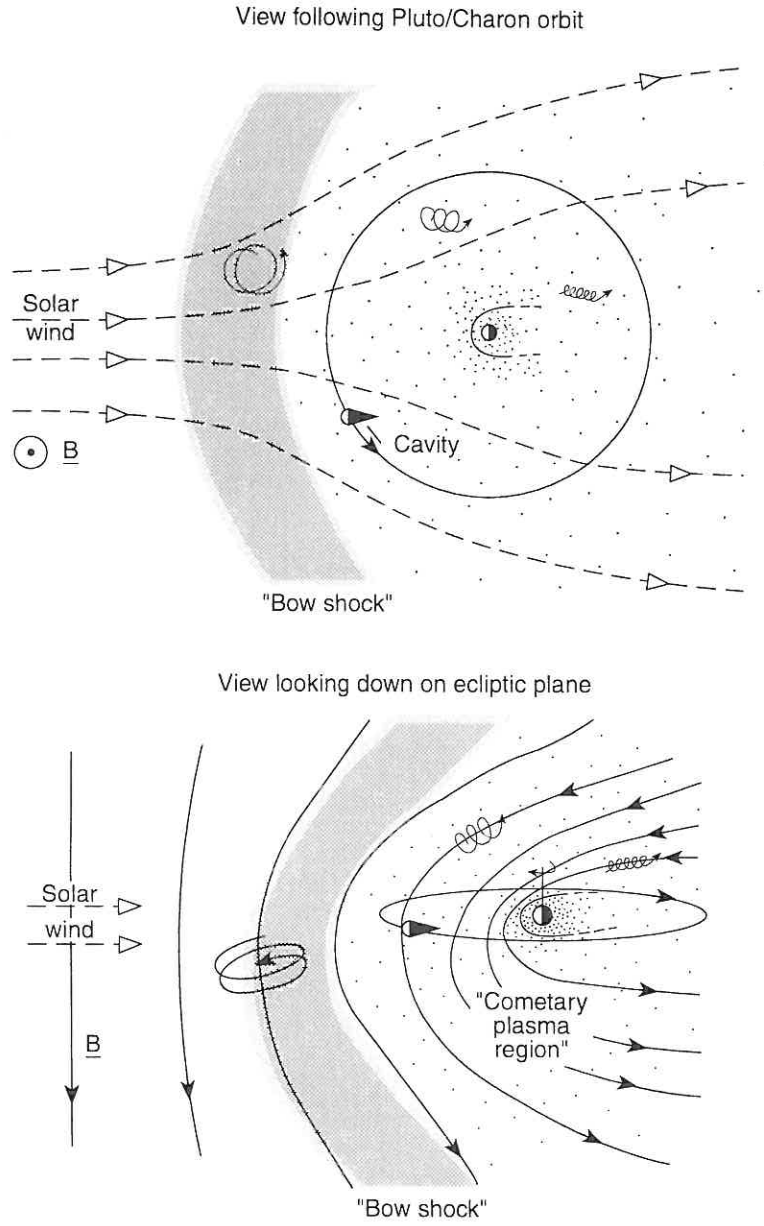

Figure 4. Sketch of the interaction of Pluto with the solar wind for the case of a strong atmospheric escape rate. The solid (dashed) arrows show magnetic field lines (solar wind flow). The orbit of Charon is shown to scale. The trajectories of cometary pickup ions are sketched as helical arrows.

As the solar wind flow penetrates the escaping neutral outflow, local ionization and subsequent pickup decelerates the solar wind, leading to stagnation when the newly picked up cometary ions dominate the composition (at $\sim R_{so}/3$ according to Galeev et al. [1985]). In the cometary plasma region the flow speeds are reduced to a few km s^{-1}, the magnetic field is compressed, collisions become increasingly frequent and charge exchange cools the plasma. In this "pile-up" region the magnetic pressure is roughly equal to the upstream ram pressure. From Galeev et al. (1985)

$$B_{max} = (2\mu_o \rho_{sw} V_{sw}^2)^{1/2} \quad (6)$$

which at Pluto would be ~1.5 nT. In a 1.5 nT field CH_4^+ ions of just 1 eV have a gyroradius of 272 km, about 1/4 R_{Pluto} (which is much smaller than the size of the pile-up region so that the MHD-based cometary models are valid). Thus, field lines will be hung up and draped around Pluto, in a manner similar to a comet.

A major difference between Pluto and a comet is the larger size of the planet compared with a comet nucleus (~10 km). The cometary plasma region extends inwards, collecting cooler, denser, more slowly moving plasma until the point is reached (at the collisionopause) where collisions between expanding neutrals and the plasma electrons are more frequent than $1/t$ where t is the time an electron takes to transit the region (Mendis et al. 1986; Cravens et al. 1987). For comet G-Z the collisionopause is estimated to be located at ~2000 km. For Pluto, our cometary model breaks down at the exobase, which is rather difficult to locate under the classical definition (where $\int_{r_c}^{\infty} n(r)\sigma dr = 1$) because neutrals are removed by the solar wind interaction. However, the value of $\lambda_1 \sim 10$ derived by McNutt (1989) for a methane atmosphere, for example, corresponds to a distance of ~2.2 R_{Pluto} for the altitude of unit optical depth, below which the cometary model is not valid. Clearly, one needs to develop a model of Pluto's atmosphere and ionosphere incorporating the interaction with the cometary plasma flow self-consistently.

V. IONOSPHERIC INTERACTION

If the atmospheric escape flux is less than 1.5×10^{27} molecules s^{-1} then the solar wind will interact more directly with the planet's atmosphere (see Fig. 5), similar to the cases at Venus and Mars and to the magnetospheric interaction with Titan. Figure 5 illustrates the generic interaction of a flowing plasma with an atmosphere. The Venus case is the best studied because of the extensive Pioneer Venus data but, as we discuss below, the cases of Mars or Titan are probably more appropriate analogies.

The Pioneer Venus Orbiter (PVO) provided a fairly detailed picture of the solar wind interaction with a planetary ionosphere (see, e.g., Luhmann 1986). PVO observations showed that the Venus ionosphere acts as an effective obstacle in the solar wind flow because the thermal pressure of the ionosphere

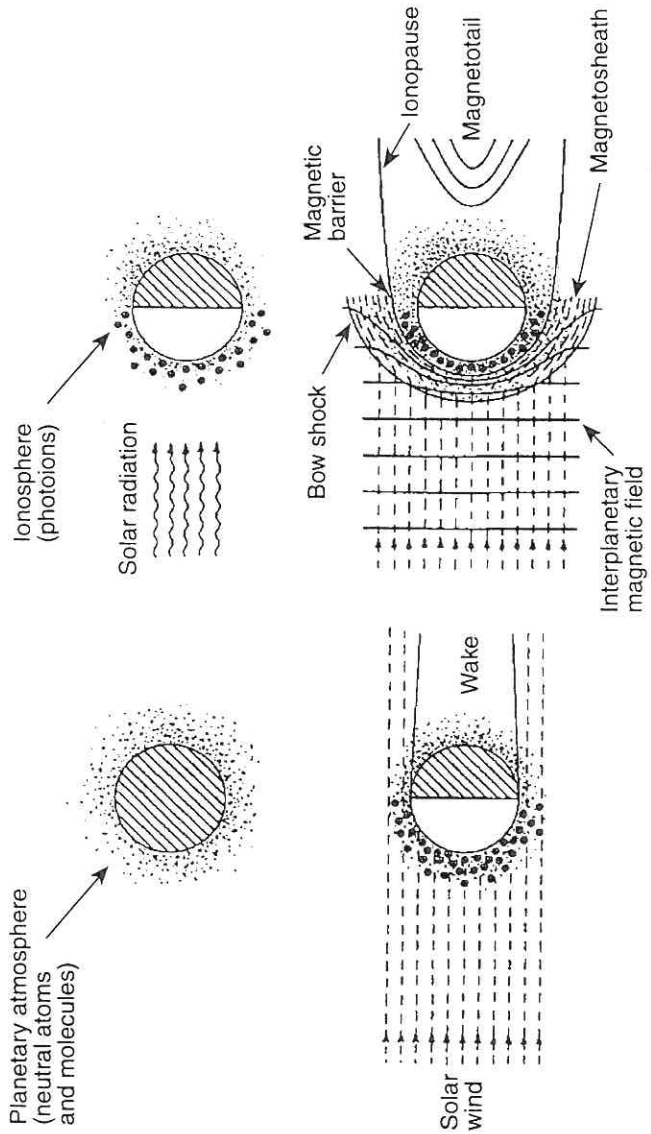

Figure 5. Processes involved in the interaction of the solar wind with a static atmosphere.

usually exceeds the incident solar wind dynamic pressure. An ionopause boundary forms at ~300 km altitude above the surface of Venus where the two pressures become equal. This boundary appears to separate the ionospheric plasma from the solar wind plasma. Currents flow in this boundary, much as they flow on the magnetopause of a planetary magnetosphere. These currents produce a magnetic barrier that diverts the solar wind around the bulk of the ionosphere below. The ionopause moves up and down in response to changes in the solar wind pressure. When the ionopause is in a collisionless part of the ionosphere, it is about one thermal ion gyroradius thick (i.e., a few tens of km). When the solar wind pressure is high, the ionopause moves down into the collisional region of the ionosphere and the IMF diffuses in, thus producing a thicker boundary layer whose scale is determined by scale heights and thermal and magnetic pressure gradients. Moderate amounts of heavy planetary ions picked up from the upper atmosphere above the ionopause (mainly oxygen at Venus) cause an induced magnetotail to form in the wake.

Consideration of whether Pluto can have a Venus-like solar wind interaction depends in part on the properties of its ionosphere which are unknown. If one considers a simple Chapman layer where the production of electrons by photoionization balances recombination losses in an isothermal atmosphere, then the height of maximum electron density is given by (see, e.g., Chamberlain and Hunten 1987)

$$h_m = H \log(\sigma H_o n_o). \tag{7}$$

Taking $\sigma \sim 4 \times 10^{-18}$ cm^2, $n_o \sim 8.3 \times 10^{13}$ cm^{-3} and $H_o \sim 60$ km, then $h_m \sim 7.6\ H \sim 1.4\ R_{Pluto}$ (allowing for the increase in H due to the decreasing gravity with altitude). For a nonisothermal atmosphere the effective scale height would be much less, reducing the altitude of the electron density peak. Extrapolating solar EUV fluxes from 1 AU for solar minimum/maximum (see, e.g., Cravens et al. 1987), one gets values of $F_\nu \sim 2 \times 10^7$ to 2×10^8 photons cm^{-2} s^{-1} at 30 AU, which give peak electron production rates of

$$q_m = \frac{F_\nu}{He^{-1}} \approx 9 - 90 \text{ cm}^{-3} \text{ s}^{-1}. \tag{8}$$

The composition of Pluto's ionosphere depends on the composition of its upper atmosphere. The two major species in the neutral atmosphere are expected to be molecular nitrogen and methane. These also happen to be the major neutral species in both Titan's and Triton's atmospheres, so we can draw on our understanding of the ionospheric composition and chemistry of those two ionospheres (cf., Keller et al. 1992; Cravens et al. 1992; Ip 1990; Yung and Lyons 1990; Majeed et al. 1990) to learn about Pluto's ionosphere. The ionospheres of Triton and Titan appear to be quite different in spite of the very similar composition of the lower atmospheres. In the case of Titan, the relative abundance of methane in the thermosphere in the vicinity of the ionospheric peak is approximately 10% (cf., Keller et al. 1992; Yung 1987), whereas in the case of Triton the relative abundance of methane in the upper atmosphere

appears to be less than a part per million. Although the lower atmosphere of Pluto contains both N_2 and CH_4, there are two scenarios to consider and they depend upon the relative amount of methane present. A significant amount produces a Titan-like ionosphere and a trace amount of methane would result in a more Triton-like ionosphere. We consider the Titan-like case first.

The main ions produced via photoionization, or by electron impact, will be N_2^+ and CH_4^+, although some N^+, CH_3^+, and CH_2^+ ions should also be produced. However, the major ion species are *not* expected to be N_2^+ or CH_4^+. Ion-neutral chemistry will alter the ion composition. In a pure CH_4 atmosphere, methane ions will undergo the following rapid reaction:

$$CH_4^+ + CH_4 \rightarrow CH_5^+ + CH_3. \tag{9}$$

The major ion species will be CH_5^+. The CH_5^+ ions will recombine dissociatively with a rate coefficient of $\alpha \approx 10^{-6}$ cm^3 s^{-1} for electron temperatures less than about 1000 K.

For Pluto's atmosphere, containing both N_2 and CH_4, the following ion-neutral reactions become important (cf., Keller et al. 1992):

$$N_2^+ + CH_4 \rightarrow CH_3^+ + N_2 + H \tag{10}$$

$$CH_3^+ + CH_4 \rightarrow C_2H_5^+ + H_2. \tag{11}$$

This leads to $C_2H_5^+$ being a major ion species. In fact, if no significant abundance of the neutral species HCN is present, then $C_2H_5^+$ will probably be the major ion species. However, HCN is produced via neutral photochemistry in Titan's mesosphere and thermosphere (Yung et al. 1984)—and could also probably be produced in the upper atmosphere of Pluto—and although it remains a minor neutral species, its participation in the following reaction means that it has an important effect on the ion composition:

$$C_2H_5^+ + HCN \rightarrow H_2CN^+ + C_2H_4. \tag{12}$$

The H_2CN^+ ion recombines dissociatively as does $C_2H_5^+$. Keller et al. (1992) also demonstrated that heavier hydrocarbon ions are likely to be present in Titan's ionosphere as well.

We expect then that, if Titan provides a reasonable analogy, the ionosphere of Pluto will primarily be composed of a combination of CH_5^+, $C_2H_5^+$, and H_2CN^+ ions, all of which will dissociatively recombine with $\alpha \approx 10^{-6}$ cm^3 s^{-1}. The Pluto ionosphere is likely to be photochemically controlled near its peak with an electron density given by the following photochemical expression:

$$n_{e,\max} \approx [q_m/\alpha]^{1/2} \approx 0.5 - 1 \times 10^4 \text{ cm}^{-3} \tag{13}$$

which is approximately the value also predicted for Titan. The ionospheric thermal pressure, $p = n_e k(T_e + T_i)$, has a maximum value of roughly 1 to

2×10^{-9} dyne cm^{-2} using $n_{e,\max}$ and $T_e \approx T_i \approx 10^3$ K. This value of T_e is reasonable for the peak region of the ionosphere, by analogy with Titan (Gan et al. 1992).

The other possibility is that the methane on Pluto is only present in trace amounts and the atmosphere is more similar to that of Neptune's moon Triton. Triton has mostly N_2 with CH_4 present in only trace amounts (Broadfoot et al. 1989). CO is limited to $\ll 1\%$ of N_2 by the observations. Support for this scenario is enhanced by recent observations of surface ices by Owen et al. (1993).

The Voyager 2 radio science experiment (Tyler et al. 1989) observed a Triton ionosphere with a peak n_e of about 2×10^4 cm^{-3}, which is almost a factor of 10 higher than the upper limit set for the ionosphere of Titan. Ip (1990), Yung and Lyons (1990) and Majeed et al. (1990) all conclude that to explain the high observed electron densities the major ion must be N^+ rather than a molecular ion which can recombine rapidly. It was suggested that due to the low abundance of methane at ionospheric altitudes the molecular nitrogen ions do not react with CH_4 (as they do at Titan) but instead dissociatively recombine (i.e., $N_2^+ + e^- \rightarrow N + N$) or react with H_2 to produce N_2H^+, which also dissociatively recombines (Majeed et al. 1990). More importantly, about 10% of photoionization or electron impact ionization events for N_2 are dissociative, leading to the production of N^+ ions. On Titan, these N^+ ions are rapidly removed by reaction with CH_4, so that the N^+ density is low, but on Triton N^+ is the major ion and the density is quite high because the main loss processes for this atomic ion (radiative recombination or reaction with H_2) are quite slow. Hence, if Pluto has a low methane abundance in its upper atmosphere, then N^+ is likely to be the major ion species and the peak electron density may actually be higher than in the Titan scenario ($n_{e,\max} = 2 \times 10^4$ cm^{-3}). In this case, Pluto's maximum ionospheric pressure will be 4×10^{-9} dyne cm^{-2} (a few times higher than at Titan).

To summarize, the current consensus is that N^+ dominates Triton's ionosphere although electron precipitation from the magnetosphere of Neptune appears to play a primary role in determining the ionospheric structure (Strobel et al. 1990; Ip 1990; Yung and Lyons 1990; Majeed et al. 1990). So, if methane is present in only trace amounts in Pluto's atmosphere as recent (indirect) measurements suggest (Stern et al. 1993; Owen et al. 1993), then Pluto's ionosphere may resemble that of Triton albeit without magnetospheric electron input. In this case, N_2 is ionized to yield both N^+ and N_2^+. The molecular nitrogen ions recombine fairly rapidly while the atomic nitrogen ions will dominate the ionosphere due to their much longer radiative recombination times.

In any case, the expected ionospheric pressure is small, but it still exceeds the ram pressure of the solar wind at 30 AU, $2.2(\pm 1.8) \times 10^{-11}$ dyne cm^{-2} assuming a 5% admixture of α-particles in the solar wind (Belcher et al. 1993). Thus, one expects a large interaction region compared with the size of the planet, with $R_{\text{ionopause}} \sim 1.5\ R_{\text{Pluto}}$ (for the Titan-like case). This is

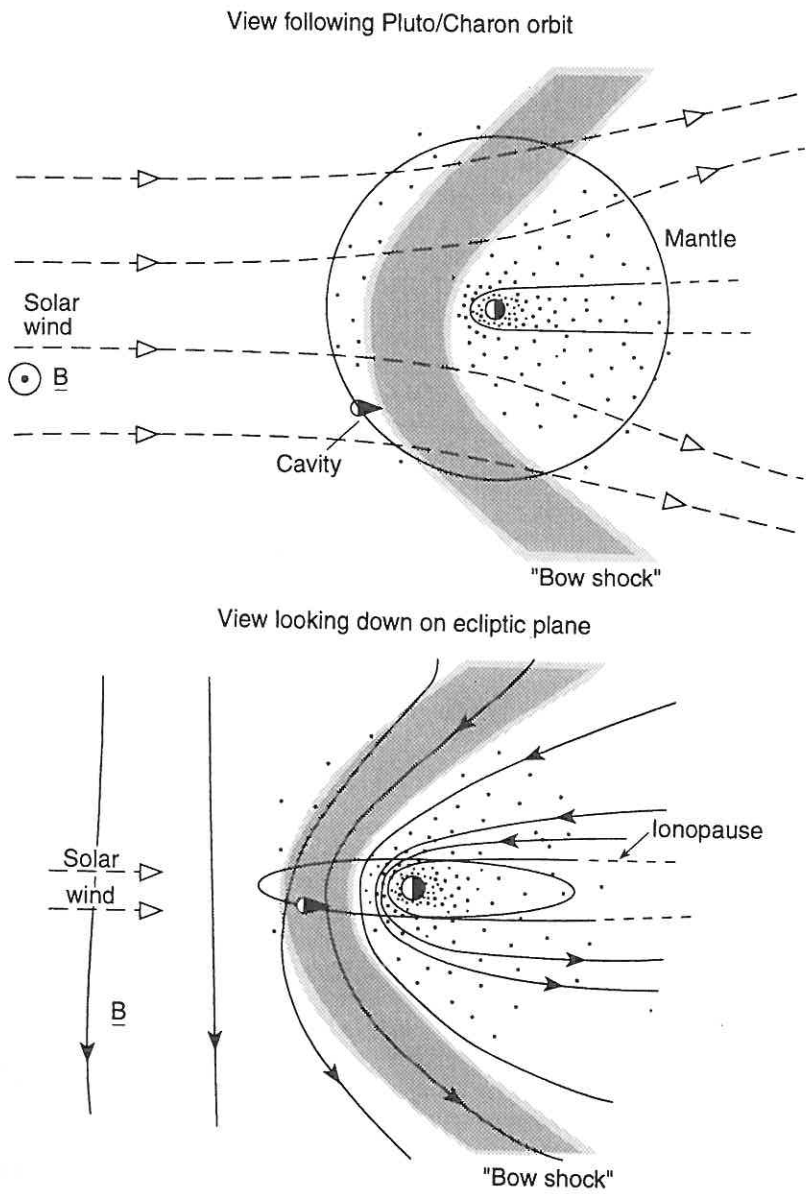

Figure 6. Sketch of the interaction of Pluto's ionosphere with the solar wind for the case of a weak atmospheric escape rate. The solid arrows show magnetic field lines. The dots indicate the extended neutral atmosphere.

actually more reminiscent of Titan where $R_{ionopause} \sim 1.4$ to 1.8 R_T (Hartle et al. 1982; McNutt and Richardson 1988) than Venus (where $R_{ionopause} \sim 1.03\ R_V$ according to Luhmann [1986]) and Mars (where $R_{ionopause} \sim 1.15\ R_M$ according to Luhmann [1992]). Nevertheless, the question of a Venus-like interaction is worth exploring as we have far more knowledge of the Venus example than the Mars or Titan examples.

At Venus, where the average IMF strength is ~13 nT and the ionopause obstacle is about 0.3 R_V from the subsolar bow shock (1 R_V = 6053 km), the solar wind protons have gyroradii much smaller than the subsolar magnetosheath thickness. This scaling allows the bulk of the shocked solar wind protons to move in a manner approximating an MHD fluid (cf., Luhmann 1992). PVO observations suggest that most of the solar wind plasma flows smoothly around an obstacle slightly larger than the observed ionopause (Zhang et al. 1991). In the absence of substantial comet-like "mass loading" of the solar wind near Pluto by planetary pickup ions, the nominal distance of a planetary bow shock for an upstream flow Mach number of ~10 is only ~1.2 times the obstacle nose radius (Stahara et al. 1980). The gyroradius of a solar wind proton that would result from full conversion of its flow energy to thermal energy at a subsolar quasi-perpendicular shock would be at least several R_{Pluto} (assuming 1 keV protons in a 0.2 nT field that quadruples in strength at the shock). Thus, it is unlikely that anything resembling the Venus–solar wind interaction observed by PVO occurs at Pluto. Any tendency to form a Venus-like magnetosheath would be thwarted by the large size of the proton gyroradii relative to the estimated (1.5 R_{Pluto}) Pluto ionopause nose radius.

The case of Pluto may be more akin to the interaction of Mars (see, e.g., Moses et al. 1988; Brecht et al. 1993), where a conventional subsolar bow shock does not seem to form due to the lack of adequate space for thermalization of the shocked solar wind proton distribution in the downstream magnetosheath. Part of the inferred scenario for Mars is a departure from fluid-like diversion of the solar wind plasma around the ionopause obstacle (see, e.g., Brecht and Ferrante 1991) with the implication that some solar wind is absorbed below the obstacle surface.

Of course, the presence of even a weak extended upper atmosphere affects this simple picture, as it does at both Venus and Mars. At Venus, most of the mass loading of the solar wind by ionospheric ions seems to originate in the inner magnetosheath, where it has minimal effect on the bow shock but still leads to the formation of the induced magnetotail (see, e.g., Luhmann 1986). At Mars, the more extended exosphere due to the lower Martian gravity may have more significant consequences on the solar wind interaction, but the nature and extent of these remains a subject of current research. At least the gross features of the Mars solar wind interaction, including the induced magnetotail, seem similar to those at Venus (see, e.g., Luhmann et al. 1991). The exception is the more turbulent looking subsolar shock and magnetosheath that apparently result from the ion kinetic effects (Brecht et al. 1993).

Figure 6 is a sketch of the solar wind interaction with Pluto's atmosphere for low atmospheric escape rates. Note that scavenging of the atmosphere via solar wind sputtering could significantly deplete the volatile reservoir over the planet's lifetime (see Kass and Yung [1995] for discussion of this issue at Mars).

VI. SURFACE IRRADIATION EFFECTS

There is some evidence that Pluto has reddened over the past 40 years (Stern et al. 1988; Buie and Tholen 1989; chapter by Buie et al.). Given current speculation about the nature of Pluto's interaction with the solar wind, it seems worthwhile to explore whether magnetospheric effects could have led to possible color changes as Pluto approached perihelion during this century (see Johnson [1990] for general discussion of irradiation effects on planetary materials).

Bombardment of methane ice by energetic (10 keV to 100 keV) protons leads to carbon enrichment, and hence darkening of the ice-bearing material, for fluences greater than 10^{16} cm^{-2}. Such irradiation has been suggested to be responsible for the dark color of the moons and rings of Uranus (Lanzerotti et al. 1987). Thompson et al. (1987) note that significant color changes of methane clathrate occur for radiation doses of 10^9 erg cm^{-2}. They further note that the coloration of both Pluto and Triton suggests irradiated ice cover on the respective surfaces with color persistence suggesting resurfacing on time scales similar to those required for accumulation of a 10^{10} erg cm^{-2} charged-particle dose; differences in the Pluto and Triton spectra suggest the visibility of a greater amount of irradiated material at Pluto. Since these remarks were made, Triton has been found to have an essentially N_2 atmosphere with a surface temperature and pressure of 38 K and 14 μbar, respectively, with a thermospheric temperature of 90 K (Strobel et al. 1990 and references therein). In addition, Strobel et al. (1990) note that the ionosphere of Triton is produced by the precipitation of $\gg$10 keV electrons to an extent that the ionosphere is an excellent electrical conductor, shielding the moon from the direct access of Neptunian magnetospheric plasma.

From 1977 to 1989 Triton grew less red, presumably due to the atmospheric deposition of fresh nitrogen frost on radiation damaged methane clathrate, although the change was rather rapid and puzzling in other details as well (McEwen 1990). The opposite color change (cf., the reddening of Pluto) could also be due to movement of surface frosts or could be an irradiation effect. This latter case can only occur if the particle fluxes are sufficiently high, however.

Johnson (1989) has considered the effects of various sources of radiation on the surface properties of Pluto. He notes: "...in the absence of any local particle precipitation, the amount of darkening occurring in one orbit is small." Changes in the albedo over an orbit would then have to be the result of atmospheric dynamics in covering and uncovering material radiation darkened over cosmogonic time scales (see the chapter by Spencer et al.).

For pickup ions in the solar wind, one expects a characteristic energy of up to $\mu\, m_p\, V_{sw}^2$ where m_p is the proton mass, V_{sw} the solar wind speed, taken as ~400 km s^{-1}, and μ is the mass in amu of the ion under consideration (assumed to be singly ionized). At Pluto one expects μ~15 for the dominant ion and significant pickup fluxes of $\sim 2 \times 10^2$ cm^{-2} s^{-1} keV^{-1} up to 10 keV for an outgassing rate of $Q \sim 10^{28}$ s^{-1} (Kecskemety and Cravens 1993).

From Yelle and Lunine (1989) we assume that the temperature is 106 K at the 1 μbar level. Then, combined with a scale height of 60 km, this yields a column density of 4×10^{20} cm^{-2}. For ions to penetrate to this level losing only less than half of their energy implies an initial energy of 115 keV, about a factor of 10 greater than the nominal pickup energy. Kecskemety and Cravens (1993) have shown that negligible fluxes are accelerated to these energies in a strictly comet-like interaction. Argued from a different point of view, 10 keV ions will penetrate to 0.02 μbar. A flux of 10^3 cm^{-2} s^{-1} ions would deliver 4×10^{-6} erg cm^{-2} s^{-1}, which is less than 1% of the expected energy input (at higher levels) by solar EUV (McNutt 1989 and references therein).

For a mean ion (or electron) energy of 150 keV, significant darkening over 150 yr, e.g., roughly half an orbit, would require a flux of 10^9 erg cm^{-2}/150 keV/150 yr $\sim 9 \times 10^5$ cm^{-2} s^{-1}. Such fluxes would only be possible with an intrinsic magnetosphere interacting with the solar wind and even then are on the high side. Given our current state of knowledge of the Pluto-Charon system, it appears unlikely that changes in planetary coloring over an orbital period are the result of surface irradiation. Stern et al. (1988) reached similar conclusions.

To summarize, there is some evidence for the reddening of Pluto as it approached perihelion this century. Methane frost is known to be present on the surface; it is also present on other outer solar system bodies. Radiation from magnetospheric particles at Uranus and Neptune have led to reddening/darkening of moon and ring material in those systems. If Pluto undergoes a comet-like interaction, pickup ions will be produced in the upstream solar wind which can impact Pluto's atmosphere. (If the interaction region is sufficiently large they will also impact Charon, as we have noted elsewhere.)

However, the energies of the ions are not apparently sufficient to reach Pluto's surface at this time. As the outgassing rate decreases, penetration of ions to the surface will increase, but their intensity will drop. Hence, the reddening does not appear to occur as an induced magnetospheric effect. If Pluto possesses an intrinsic magnetic moment high enough to provide an intrinsic magnetosphere, then sufficient fluxes of sufficiently energetic ions and electrons may be present to affect the surface color. However, M. G. Kivelson (personal communication) has pointed out that the solar wind energy input, or equivalently, the convection electric field is so weak that even this mechanism may not be able to energize particles sufficiently to penetrate the atmosphere.

VII. CHARON

While Elliot and Young (1991) report some controversial evidence of an atmosphere of Charon, it is likely to be tenuous (because Charon's gravity is weak) and transient (because there is no evidence of surface volatiles to replenish any escaping atmosphere) (see the chapter by Yelle and Elliot). Furthermore, unless Pluto has a strong-enough magnetic field to produce a magnetosphere extending to Charon's orbit, any atmosphere of Charon will become ionized and removed by the solar wind. Charon should be considered, therefore, as a solid object immersed in a flowing plasma.

If Charon has any appreciable remanent magnetization, one would expect Pluto to have the greater magnetization and still dominate the electrodynamics of the system. If magnetized, Charon would nonetheless perturb the plasma medium close to the satellite. Unfortunately, there are no constraints on Charon's magnetization.

A magnetic field diffuses through an object with a time scale $\tau_d \sim \mu_o \sigma\, L^2$ where L is the size and σ the electrical conductivity of the body. If this diffusive time scale is much less than the time scale for changes in the ambient magnetic field then the field passes through the body largely unperturbed. For a magnetic field "frozen" into a plasma flowing at a characteristic speed V, the object sees the field change over the convective time scale $\tau_c \sim L/V$. Hence the magnetic interaction is weak for a nonconducting body with low magnetic Reynolds number ($R_m = \tau_d/\tau_c = \mu_o \sigma L V \ll 1$). For Charon, which has a radius of about 600 km and whose ice/rock interior is probably less conductive than that of Pluto, R_m is half that of Pluto, at best. Without its own atmosphere, Charon has no bound ionosphere to act as a conducting barrier. Hence, if neither body is intrinsically magnetized, the local ambient magnetic field is probably not affected by Charon's presence.

Although magnetic fields readily diffuse through a nonconducting body, the plasma particles obviously cannot penetrate the body and are therefore absorbed. Because the flowing plasma is absorbed on the upstream surface, there is a cavity behind the object and a wake is formed downstream as the plasma expands into the low pressure region. The Earth's Moon and most of the icy satellites of the outer planets are nonconductors and hence simple absorbers of the flowing plasma in which they are embedded (see, e.g., Ness et al. 1967).

If Pluto's atmospheric escape rate is low, then Charon is embedded in the solar wind, receiving 2×10^4 to 2×10^6 protons cm^{-2} s^{-1} (of kinetic energy ~1 keV). For expected atmospheric escape rates from Pluto Kecskemety and Cravens (1993) calculate that the density of pickup fluxes at Charon's orbit should be at least ~10 ions cm^{-2} s^{-1} keV^{-1} for methane pickup ions of 10 to 40 keV. Both these pickup ion fluxes and the solar wind proton flux would sputter material from the surface of Charon. For a pickup distribution ~5 keV wide, the sputtering fluxes are ~50 ions cm^{-2} s^{-1}. Using an optimistic sputtering yield of ~5 gives $\sim 3.5 \times 10^{26}$ molecules yr^{-1} or about 10 kg of

sputtered water over the course of a year. This additional source of material would contribute to the local mass loading and general escape of material from the Pluto–Charon system.

VIII. VARIABILITY

A. Short-Term Variability

Voyager and Pioneer measurements show that in the outer heliosphere the solar wind seems to settle into a steady pattern of a strong stream lasting a few days and repeating each 26-day solar rotation period (Lazarus et al. 1988; Gazis et al. 1989). From a statistical study of Voyager 2 PLS data obtained over 8 months in 1988, extrapolated to 30 AU, Villanueva et al. (1989) report a solar wind flux $n_{sw}V_{sw}$ ranging from 2.1×10^4 to 1.8×10^6 cm^{-2} s^{-1} with an average of $3.6 \times 10^5 \pm 2.6 \times 10^5$ cm^{-2} s^{-1}. For a steady atmospheric escape flux (say 10^{28} s^{-1}) the corresponding 1σ variation in the size of the comet-like interaction region R_{so} is ~3.9 to 24 R_{Pluto} for time scales of a few days (comparable to Pluto's rotation and Charon's orbital period of 6.4 days). If the atmospheric escape flux is low and the solar wind impinges directly on the ionosphere, then the size of the interaction region will also change in response to the solar wind ram pressure, though less dramatically than in the cometary case (because, effectively, the ionosphere is much less compressible).

B. Long-Term Variability

Perhaps the most intriguing aspect of the Pluto–Charon system is the possibility of major changes over the 248-yr orbital period due to the high orbital eccentricity. Stern et al. (1988) propose that Pluto's current dense atmosphere will freeze out, depositing a layer of methane snow onto Pluto's surface as Pluto recedes from perihelion. If, instead, N_2 dominates the atmosphere as more recent measurements have suggested (see the chapter by Trafton et al.), the atmosphere may not completely freeze out but would undergo radical compositional changes.

In Fig. 7 we have tried to illustrate how types of solar wind interactions depend on the surface values of any intrinsic magnetic field (B_o) and the atmospheric escape flux (Q_{esc}). If Pluto has a strong magnetic field (B_o>3700 nT) then a magnetosphere will remain around Pluto and Charon throughout their orbit. The amount of magnetospheric plasma will vary, with the atmosphere of Pluto forming "a comet within a magnetic bottle" at perihelion and becoming very close to a vacuum magnetosphere at aphelion. (The comet in a bottle may bear some resemblance to the situation at Uranus; there, the extended exosphere is the primary, though weak, plasma source for that planet's magnetosphere—see McNutt et al. [1987] and Selesnick and McNutt [1987].)

In the absence of a significant intrinsic magnetic field one might expect that the solar wind interaction at Pluto might undergo a transition from "cometary" to "planetary" to "lunar" behavior as the escape flux decreases,

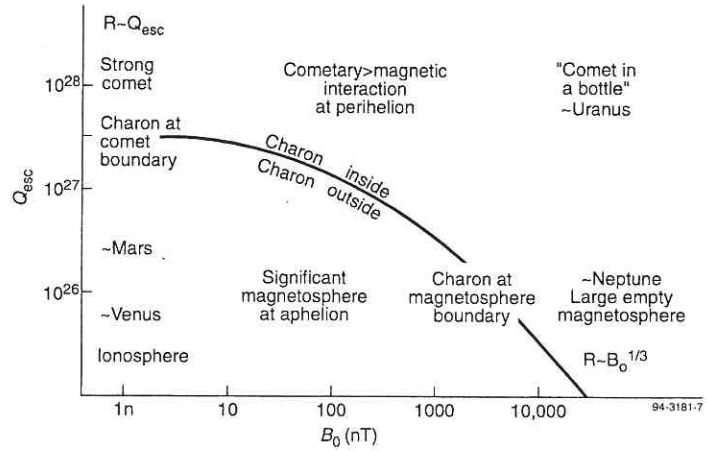

Figure 7. Types of solar wind interactions as a function of atmospheric escape rate (Q_{esc}) and instrinsic magnetic field at Pluto's surface (B_o).

though the details of how this might happen are uncertain. Indeed, it may be that the Pluto interaction never enters the "planetary" regime. If the bow-shock distance predicted for the cometary interaction always exceeds the 1.2 $R_{ionopause}$ distance predicted from the ionosphere model, and the ionosphere ceases to provide adequate thermal pressure as the mass loading weakens on receding from the Sun, then the Pluto interaction may evolve directly from comet-like to Moon-like. The resolution of this question requires more sophisticated models that determine the coupled atmosphere, ionosphere and surface properties as a function of heliocentric distance.

If Pluto has no intrinsic magnetic field, then at aphelion, if the atmosphere has frozen out, one expects the situation sketched in Fig. 8 where both Pluto and Charon have lunar-like interactions with the solar wind, entailing the diffusion of the IMF through the nonconducting bodies and absorption of the solar wind (typical fluxes dropping by a half between 30 and 50 AU) on the sunlit side, generating what must be the closest one gets in the solar system to a complete vacuum in the cavity behind.

Finally, we mention a recent study by Shimazu and Terasawa (1995) of electromagnetic induction heating of meteorites during periods of exceptionally strong solar winds (such as in the T Tauri phase of the Sun). They found that the surface is nonuniformly heated, particularly for objects at large distances from the Sun where low temperatures lead to low conductivities and hence higher heating rates. It is possible that such electromagnetic induction heating may have had a significant effect on the thermal evolution of Pluto and Charon.

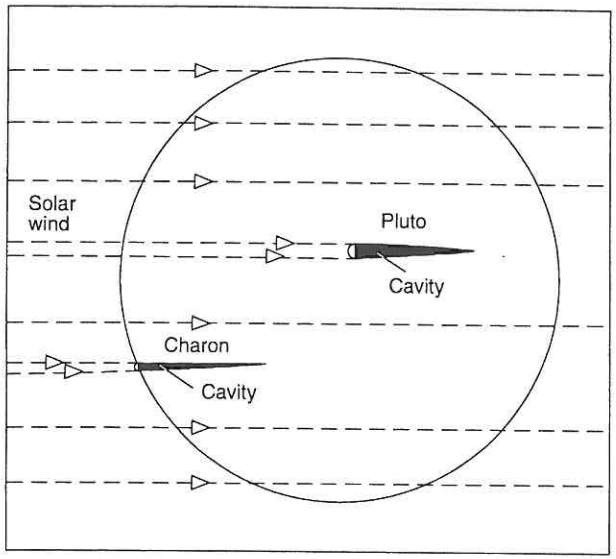

Figure 8. Sketch of the interaction of Pluto with the solar wind at aphelion. The dashed arrows show the solar wind flow.

IX. FUTURE SPACECRAFT MEASUREMENTS

Pluto's large distance from Earth, the tenuous nature of its atmosphere and the weak solar wind at 30 AU make it unlikely that the unique plasma environment of the Pluto–Charon system can be observed remotely. It is therefore interesting to consider what measurements might be made by a spacecraft passing through the system. The main objectives would be to measure the strength of Pluto's magnetic field, the extent of the atmospheric escape and the basic nature of the solar wind interaction with Pluto, both for its own sake and for comparative magnetospheric studies. Moreover, measurement of the composition of the upstream pickup ions or products from the sputtering of Charon would permit the determination of the composition of Pluto's atmosphere and/or Charon's surface. Additionally, one would need to observe the unperturbed upstream solar wind environment to measure the plasma input to the system.

In the case of the magnetic interaction, the signatures to look for are the existence of a magnetospheric boundary, the magnetopause, where the plasma composition and velocity distributions dramatically change and for specific emissions of plasma waves and radio waves. In the case of a cometary interaction, the distinctive signatures are the presence of pickup ions well upstream of Pluto, the deceleration of the solar wind over a substantial region, a weak bow shock farther from Pluto and high levels of waves and turbulence

in the cometosphere. In the case of a weaker atmospheric escape rate and an ionospheric interaction with the solar wind, we expect to see a strong bow shock signature at 1.2 to 1.5 R_{Pluto}, few pickup ions in the upstream region and a tail of suprathermal pickup ions in the wake. Beams of energetic ions may also be seen on field lines magnetically connected to the bow shock. Figure 9 shows a Pluto flyby trajectory on the same scale as the Voyager flyby of Titan.

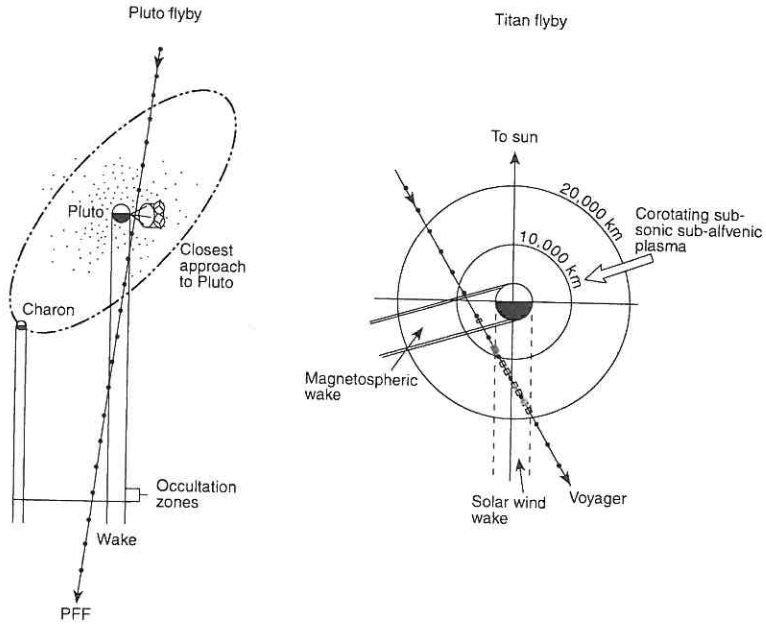

Figure 9. Comparison of spacecraft flybys of Pluto–Charon and Titan.

To distinguish between these different types of interactions and to determine the nature of the processes governing them, it is necessary to measure the following: the density (0.005 to 1 cm^{-3}) and velocity distribution of solar wind protons (50 to 600 km s^{-1}); the fluxes of pickup ions (with speeds $<$1200 km s^{-1}); waves (up to 50 kHz); the mass spectrum of pickup ions (1–4, 12–15, 16–19, 26–33 and 40–45 amu/charge); magnetic fields (0.1 to several hundred nT); fluxes of energetic particles (up to ~MeV/nucleon); and the electron spectrum (from 10^2–10^6 eV). A small payload of just three instruments, a combined particle detector, a wave detector and a magnetometer (with a total mass of approximately 2 kg) could probably achieve such objectives on a trajectory through the system such as that shown in Fig. 9 (Neugebauer et al. 1993).

X. SUMMARY

1. While it is improbable that Pluto has an internal magnetic dynamo, even weak remanent magnetization could produce a significant magnetosphere in the weak solar wind at 30 AU. A surface field of 1 nT will stand off the solar wind from the planet's surface while ~3700 nT will produce a magnetosphere encompassing Charon's orbit. Such surface fields could be obtained if Pluto retains a remanent magnetization comparable to chondritic meteorites.

2. Pluto's low gravity results in the atmosphere being only weakly bound to the planet. Current estimates for the atmospheric escape rate range from 2.3×10^{27} to 3.4×10^{28} molecules s^{-1} (see the chapter by Trafton et al.). For typical solar wind conditions at 30 AU, escape rates significantly greater than $Q_o \sim 1.5\ 10^{27}$ molecules s^{-1} lead to upstream mass loading of the solar wind and a comet-like interaction, possibly extending beyond the orbit of Charon at 17 R_{Pluto}.

3. Because of the weak interplanetary magnetic field, ions picked up upstream of Pluto will have large gyroradii (300–600 R_{Pluto}). The fluxes of these pickup ions will be asymmetric about Pluto, the solar wind carrying them past Pluto and downwind, away from the Sun.

4. If the escape rate is less than Q_o then estimated ionospheric electron densities of 2.4×10^3 to 2.2×10^4 should be sufficient to stand off the solar wind at an ionopause distance $R_{ionopause} \sim 1.5\ R_{Pluto}$. Hence the interaction will be like that at Mars, Venus and Titan in the limiting case of low atmospheric escape flux and high solar wind flux.

5. In any case, the weak interplanetary magnetic field suggests that the thickness of an upstream bow shock will be $>10\ R_{Pluto}$, comparable to the size of the interaction region. Hence a distinct bow shock is unlikely and kinetic effects must be included in order to model the solar wind interaction realistically.

6. The large variations in the solar wind flux that are observed in the outer heliosphere suggest comparable changes occur in the size of the interaction region. For an atmospheric escape rate of $\sim 10^{28}$ s^{-1} the stand-off distance would vary from 3.9 to 24 R_{Pluto} on time scales of days.

7. Major changes in the nature of the interaction with the solar wind are expected if the atmosphere freezes out as Pluto recedes from the Sun after perihelion, as predicted by Stern et al. (1988). Around aphelion the interaction of the solar wind with both Pluto and Charon is limited to absorption of the solar wind onto the dayside hemisphere, similar to Earth's Moon if Pluto is nonmagnetic.

8. With such a tenuous medium at such a distance from the Earth, one must be extremely optimistic to believe that the nature of Pluto's interaction with the solar wind could be observed remotely. However, the extreme natures of the bow shock, the large gyroradii of upstream pickup ions, the extensive exosphere and the effects of solar wind variability make Pluto–Charon an exciting place to explore planetary plasma physics with *in-situ* measurements from a spacecraft flying close by Pluto and Charon. These fundamental exploratory measurements could be accomplished with a small particles and fields instrument package included on a focused mission such as that discussed for the Pluto Fast Flyby spacecraft (Staehle et al. 1992; chapter by Terrile et al.).

Acknowledgments. TEC was supported by a NSF grant at the University of Kansas. JGL and FB were supported by a NASA Grant. RLM and AFC were supported at the Johns Hopkins University Applied Physics Laboratory under Task I of a Navy contract.

REFERENCES

Bagenal, F., and McNutt, R. L. 1989. Pluto's interaction with the solar wind. *Geophys. Res. Lett.* 16:1229–1232.

Bagenal, F., Belcher, J. W., Sittler, E. C., and Lepping, R. P. 1987. The Uranian bow shock: Voyager 2 inbound observations of a high Mach number shock. *J. Geophys. Res.* 92:8603.

Belcher, J. W., Lazarus, A. J., McNutt, R. L., and Gordon, G. S. 1993. Solar wind conditions in the outer heliosphere and the distance to the terminal shock. *J. Geophys. Res.* 98:15177–15183.

Brecht, S. H., and Ferrante, J. R. 1991. Global hybrid simulation of unmagnetized planets: Comparison of Venus and Mars. *J. Geophys. Res.* 96:11209–11220.

Brecht, S. H., Ferrante, J. R., and Luhmann, J. G. 1993. Three-dimensional simulations of the solar wind interaction with Mars. *J. Geophys. Res.* 98:1345–1357.

Broadfoot, A. L., Atreya, S. K., Bertaux, J. L., Blamont, J. E., Dessler, A. J., Donahue, T. M., Forrester, W. T., Hall, D. T., Herbert, F., Holberg, J. B., Hunten, D. M., Krasnopolsky, V. A., Linick, S., Lunine, J. I., McConnell, J. C., Moos, H. W., Sandel, B. R., Schneider, N. M., Shemansky, D. E., Smith, G. R., Strobel, D. F., and Yelle, R. V. 1989. Ultraviolet spectrometer observations of Neptune and Triton. *Science* 1459–1466.

Buie, M., and Tholen, D. J. 1989. The surface albedo distribution of Pluto. *Icarus* 79:23–37.

Chamberlain, J. W., and Hunten, D. M. 1987. *Theory of Planetary Atmospheres* (New York: Academic Press).

Coates, A. J., Johnstone, A. D., Huddleston, D. E., Wilken, B., Jockers, K., Borg, H., Amata, E., Formisano, V., Bavassano-Cattaneo, M. B., Winningham, J. D., Gurgiolo, C., and Neubauer, F. M. 1993*a*. Pick-up water group ions at Comet Grigg-Skjellerup. *Geophys. Res. Lett.* 20:483–486.

Coates, A. J., Johnstone, A. D., Wilken, B., and Neubauer, F. M. 1993*b*. Velocity space diffusion and non-gyrotropy of pickup water group ions at comet Grigg-Skjellerup. *J. Geophys. Res.* 98:20985–20994.

Cravens, T. E., Kozyra, J. U., Nagy, A. F., Gombosi, T. I., and Kurtz, M. 1987. Electron impact ionization in the vicinity of comets. *J. Geophys. Res.* 92:9341–9353.

Cravens, T. E., Keller, C. N., and Gan, L.. 1992. The ionosphere of Titan and its interaction with Saturnian magnetospheric electrons. In *Proceedings of a Symposium on Titan*, ESA SP-338, p. 273.

Delitsky, M. L., Eviatar, A., and Richardson, J. D. 1989. A predicted Triton plasma torus in Neptune's magnetosphere. *Geophys. Res. Lett.* 16:215.
Dessler, A. J., and Russell, C. T. 1980. From the ridiculous to the sublime: The pending disappearance of Pluto. *Eos: Trans. AGU* 61:690.
Dryer, M., Rizzi, A. W., and Shen, W.-W. 1973. Interaction of the solar wind with the outer planets. *Astrophys. Space Sci.* 22:329–351.
Elliot, J. L., and Young, L. A. 1991. Limits to the radius and possible atmosphere of Charon from its 1980 stellar occultation. *Icarus* 89:244–254.
Elliot, J. L., Dunham, E. W., Bosh, A. S., Slivan, S. M., Young, L. A., Wasserman, L. W., and Millis, R. L. 1989. Pluto's atmosphere. *Icarus* 77:148.
Flammer, K. R., and Mendis, D. A. 1993. The flow of the contaminated solar wind at comet P/Grigg-Skjellerup. *J. Geophys. Res.* 21003–21008.
Galeev, A. A. 1987. Encounters with comets: Discoveries and puzzles in cometary plasma physics. *Astron. Astrophys.* 187:12–20.
Galeev, A. A. 1991. Plasma processes in the outer coma. In *Comets in the Post-Halley Era*, vol. 2, eds. R. Newburn, M. Neugebauer and J. Rahe (Dordrecht: Kluwer), p. 1145.
Galeev, A. A., Cravens, T. E., and Gombosi, T. I. 1985. Solar wind stagnation near comets. *Astrophys. J.* 289:807–819.
Gan, L., Keller, C. N., and Cravens, T. E. 1992. Electrons in the ionosphere of Titan. *J. Geophys. Res.* 97:12137.
Gazis, P. R., Mihalov, J. D., Barnes, A., Lazarus, A. J., and Smith, E. J. 1989. Pioneer and Voyager observations of the solar wind at large heliocentric distances and latitudes. *Geophys. Res. Lett.* 16:223.
Glassmeier, K.-H., and Neubauer, F. M. 1993. Low-frequency electromagnetic waves at comet P/ Grigg-Skjellerup: Overview and spectral charateristics. *J. Geophys. Res.* 98:20921–20935.
Glassmeier, K.-H., Motschmann, U., Mazelle, C., Neubauer, F. M., Sauer, K., Fuselier, S. A., and Acuña, M. H. 1993. Mirror modes and fast magnetoacoustic waves near the magnetic pileup boundary of comet P/Halley. *J. Geophys. Res.* 98:20955–20964.
Hartle, R. E., Sittler, E. C., Ogilvie, K. W., Scudder, J. D., Lazarus, A. J., and Atreya, S. K. 1982. *J. Geophys. Res.* 87:1383–1394.
Hubbard, W. B., Hunten, D. M., Dieters, S. W., Hill, K. M., and Watson, R. D. 1988. Occultation evidence for an atmosphere on Pluto. *Nature* 336:452.
Hubbard, W. B., Yelle, R. V., and Lunine, J. I. 1990. Nonisothermal Pluto atmosphere models. *Icarus* 84:1–11.
Huddleston, D. E., Coates, A. J., Johnstone, A. D., and Neubauer, F. M. 1993. Mass loading and velocity diffusion models for heavy pickup ions at comet Grigg-Skjellerup. *J. Geophys. Res.* 98:20995–21002.
Hunten, D. M., and Watson, A. J. 1982. Stability of Pluto's atmosphere. *Icarus* 51:665.
Ip, W.-H. 1990. On the ionosphere of Triton: An evaluation of the magnetospheric electron precipitation and photoionization effects. *Geophys. Res. Lett.* 17:1713–1716.
Johnson, R. E. 1989. Effect of irradiation on the surface of Pluto. *Geophys. Res. Lett.* 16:1233–1236.
Johnson, R. E. 1990. *Energetic Charged-Particle Interaction with Atmospheres and Surfaces* (Berlin: Springer-Verlag).
Kass, D. M., and Yung, Y. L. 1995. Loss of atmosphere from Mars due to solar wind-induced sputtering. *Science* 268:697–699.
Kecskemety, K., and Cravens, T. E. 1993. Pick-up ions at Pluto. *Geophys. Res. Lett.* 20:543–546.

Keller, C. N., Cravens, T. E., and Gan, L. 1992. A model of the ionosphere of Titan. *J. Geophys. Res.* 97:12117.
Kivelson, M. G., Slavin, J. A., and Southwood, D. J. 1979. Magnetospheres of the Galilean satellites. *Science* 205:491–493.
Kivelson, M. G., Bargatze, L. F., Khurana, K. K., Southwood, D. J., Walker, R. J., and Coleman, P. J. 1993. Magnetic signatures near Galileo's closest approach to Gaspra. *Science* 331–334.
Lanzerotti, L. J., Brown, W. L., Maclennan, C. G., Cheng, A. F., Krimigis, S. M., and Johnson, R. E. 1987. Effects of charged particles on the surfaces of the satellites of Uranus. *J. Geophys. Res.* 92:14949–14957.
Lazarus, A. J., Yedidia, B., Villanueva, L., McNutt, R. L., Jr., Belcher, J. W., Villante, U., and Burlaga, R. F. 1988. *Geophys. Res. Lett.* 15:1519.
Luhmann, J. G. 1986. The solar wind interaction with Venus. *Space Sci. Rev.* 44:241–306.
Luhmann, J. G. 1992. Comparative studies of the solar wind interaction with weakly magnetized planets. *Adv. Space Res.* 12(9):191–203.
Luhmann, J. G, Russell, C. T., Schwingenschuh, K., and Yeroshenko, Ye. 1991. A comparison of induced magnetotails of planetary bodies: Venus, Mars and Titan. *J. Geophys. Res.* 96:11199–11208.
Majeed, T., McConnell, J. C., Strobel, D. F., and Summers, M. E. 1990. The ionosphere of Triton. *Geophys. Res. Lett.* 17:1721–1724.
McEwen, A. S. 1990. Global color and albedo variations on Triton. *Geophys. Res. Lett.* 17:1765–1768.
McNutt, R. L., Jr. 1989. Models of Pluto's upper atmosphere. *Geophys. Res. Lett.* 16:1225–1228.
McNutt, R. L., Jr., and Richardson, J. D. 1988. Constraints on Titan's ionosphere. *Geophys. Res. Lett.* 15:709–712.
McNutt, R. L., Jr., Selesnick, R. S., and Richardson, J. D. 1987. Low energy plasma observations in the magnetosphere of Uranus. *J. Geophys. Res.* 92:4399–4410.
Mendis, D. A., Smith, E. J., Tsurutani, B. T., Slavin, J. A., Jones, D. E., and Siscoe, G. L. 1986. Comet-solar wind interaction: Dynamical length scales and models. *Geophys. Res. Lett.* 13:239–242.
Moses, S. L, Coroniti, F. V., and Scarf, F. L. 1988. Expectations for the microphysics of the Mars-solar wind interaction. *Geophys. Res. Lett.* 15:429–432.
Motschmann, U., and Glassmeier, K.-H. 1993. Nongyrotropic distribution of pickup ions at comet P/Grigg-Skjellerup: A possible source of wave activity. *J. Geophys. Res.* 98:20977–20983.
Ness, N. F., Behannon, K. W., Searce, C. S., and Cantarano, S. C. 1967. Early results from the magnetic field experiment on Lunar Explorer 35. *J. Geophys. Res.* 72:5769–5778.
Neubauer, F. M., Luttgen, A., and Ness, N. F. 1991. On the lack of a magnetic signature of Triton's magnetospheric interaction on the Voyager 2 flyby trajectory. *J. Geophys. Res.* 96:19171–19175.
Neubauer, F. M., Glassmeier, K.-H., Coates, A. J., and Johnstone, A. D. 1993*a*. Low-frequency electromagnetic plasma waves at comet P/Grigg-Skjellerup: Analysis and interpretation. *J. Geophys. Res.* 98:20937–20953.
Neubauer, F. M., Marschall, H., Pohl, M., Glassmeier, K.-H., Musmann, G., Mariani, F., Acüna, M. H., Burlaga, L. F., Ness, N. F., Wallis, M. K., Schmidt, H. U., and Ungstrup, E. 1993*b*. First results from the Giotto magnetometer experiment during the P/Grigg-Skjellerup encounter. *Astron. Astrophys.* 268:L5.
Neugebauer, M. 1990. Spacecraft observations of the interaction of active comets with the solar wind. *Rev. Geophys.* 28:231–252.
Neugebauer, M., Goldstein, B. E., Balsiger, H., Neubauer, F. M., Schwenn, R., and

Shelley, E. G. 1989. The density of cometary protons upstream of Comet Halley's bow shock. *J. Geophys. Res.* 94:1261–1269.

Neugebauer, M., Cheng, A. F., Cummings, A., Gloeckler, G., Kurth, W., Walker, R., Young, D., and Forman, M. 1993. Space physics objectives for the Pluto Fast Flyby mission. *Report to NASA Space Physics Division* (August).

Owen, T., Roush, T. L., Cruikshank, D. P., Eliott, J. L., Young, L. A., de Bergh, C., Schmitt, B., Geballe, T. R., Brown, R. H., and Bartholomew, M. J. 1993. Surface ices and the atmospheric composition of Pluto. *Science* 262:745–748.

Parker, E. N. 1964. Dynamical properties of stellar coronas and stellar winds. II. Integration of the heat-flow equation. *Astrophys. J.* 139:93–122.

Richardson, J. D., Belcher, J. W., Szabo, A., and McNutt, R. L., Jr. 1995. The plasma environment of Neptune. In *Neptune and Triton*, ed. D. P. Cruikshank (Tucson: Univ. of Arizona Press), pp. 279–340

Russell, C. T., Baker, D. N., and Slavin, J. A. 1988. The magnetosphere of Mercury. *Mercury*, eds. F. Vilas, C. R. Chapman and M. S. Matthews (Tucson: Univ. of Arizona Press), pp. 514–561.

Sagdeev, R. Z., Shapiro, V. D., Shevchenko, V. I., and Szego, K. 1986. MHD turbulence in the solar wind comet interaction region. *Geophys. Res. Lett.* 13:85–88.

Schmidt, H. U., Wegmann, R., and Neubauer, F. M. 1993. MHD modeling applied to Giotto encounter with comet P/Grigg-Skjellerup. *J. Geophys. Res.* 98:21009–21016.

Selesnick, R. S., and McNutt, R. L., Jr. 1987. Voyager 2 plasma ion observations in the magnetosphere of Uranus. *J. Geophys. Res.* 92:15249–15262.

Shimazu, H., and Terasawa, T. 1995. Electromagnetic induction heating of meteorite parent bodies by the primordial solar wind. *J. Geophys. Res.* 100:16923–16930.

Siscoe, G. L. 1979. Towards a comparative view of planetary magnetospheres. *Solar System Plasma Physics*, eds. C. J. Kennel, L. J. Lanzerotti and E. N. Parker (Amsterdam North-Holland), pp. 321–402.

Staehle, R. L., Abraham, D. S., Carraway, J. S., Esposito, P. J., Salvo, C. J., Terrile, R. J., Wallace, R. A., Weinstein, S. S., and Hansen, E. 1992. *Exploration of Pluto*, IAF-92-0558, 43rd Congress of the International Astronautical Federation, Aug. 28–Sept. 5, Washington, D. C.

Stahara, S. S., Klenke, D., Trudinger, B. C., and Spreiter, J. R. 1980. *Application of Advanced Computational Procedures for Modeling Solar Wind Interactions with Venus-Theory and Computer Code*, NASA CR-3267.

Stern, S. A., Trafton, L. M., and Gladstone, G. R. 1988. Why is Pluto bright? Implications of the albedo and lightcurve behavior of Pluto. *Icarus* 75:485–498.

Stern, S. A., Weintraub, D. A., and Festou, M. C. 1993. *Science* 261:1713–1716.

Strobel, D. F., Cheng, A. F., Summers, M. E., and Strickland, D. J. 1990. Magnetospheric interaction with Triton's ionosphere. *Geophys. Res. Lett.* 17:1661–1664.

Sugiura, N., and Strangeway, D. W. 1988. Magnetic studies of meteorites. In *Meteorites and the Early Solar System*, eds. J. F. Kerridge and M. S. Matthews (Tucson: Univ. of Arizona Press), pp. 595–615.

Thompson, W. R., Murray, B. G. J. P. T., Khare, B. N., and Sagan, C. 1987. Coloration and darkening of methane clathrate and other ices by charged particle irradiation: Application to the outer solar system. *J. Geophys. Res.* 92:14933–14947.

Trafton, L. 1980. Does Pluto have a substantial atmosphere? *Icarus* 44:53–61.

Trafton, L. 1990. A two-component volatile atmosphere for Pluto. *Astrophys. J.* 399:512–523.

Trafton, L. M., Stern, S. A., and Gladstone, G. R. 1988. The Pluto-Charon system: The escape of Charon's primordial atmosphere. *Icarus* 74:108–120.

Tyler, G. L., Sweetnam, D. N., Anderson, J. D., Borutzki, S. E., Campbell, J. K., Eshleman, V. R., Gresh, D. L., Gurrola, E. M., Hinson, D. P., Kawashima, N., Kursinski, E. R., Levy, G. S., Lindal, G. F., Lyons, J. R., Marouf, E. A., Rosen, P. A., Simpson, R. A., and Wood, G. E. 1989. Voyager radio science observations of Neptune and Triton. *Science* 246:1466–1473.

Villanueva, L. A., Steinberg, J. T., McNutt, R. L., Jr., Lazarus, A. J., and Belcher, J. W. 1989. Solar wind parameters upstream of Neptune. *Eos: Trans. AGU* 70:385.

Watson, A. J., Donahue, T. M., and Walker, J. C. G. 1981. The dynamics of a rapidly escaping atmosphere: Applications to the evolution of Earth and Venus. *Icarus* 48:150–166.

Wu, C. S., and Davidson, R. C. 1972. Electromagnetic instabilities produced by neutral-particle ionization in interplanetary space. *J. Geophys. Res.* 77:5399–5406.

Yelle, R. V., and Lunine, J. I. 1989. Evidence for a molecule heavier than methane in the atmosphere of Pluto. *Nature* 339:288–290.

Yung, Y. L. 1987. An update of nitrile photochemistry on Titan. *Icarus* 72:468.

Yung, Y. L., and Lyons, J. R. 1990. Triton: Topside ionosphere and nitrogen escape. *Geophys. Res. Lett.* 17:1717–1720.

Yung, Y. L., Allen, M., and Pinto, J. P. 1984. Photochemistry of the atmosphere of Titan: Comparison between model and observations. *Astrophys. J. Suppl.* 55:465.

Zhang, T. L., Luhmann J. T., and Russell, C. T. 1991. The magnetic barrier at Venus. *J. Geophys. Res.* 96:11145–11153.